

# Performance Analysis of Perovskite/CIGS Based Thin Film Solar Cell using BaSi<sub>2</sub> as BSF Layer

Tripti Yadav, Shivangi Yadav\*, Anupam Sahu

Department of Electronics and Communication Engineering, Madan Mohan Malaviya University of Technology,  
Gorakhpur 273010, India

\*Corresponding author's e-mail: shivkarnika@gmail.com

doi: <https://doi.org/10.21467/proceedings.161.2>

## ABSTRACT

The goal of this research is to analyse conversion efficiency (CE) of proposed copper indium gallium di-selenide (CIGS) thin film solar cell (TFSC) by incorporating perovskite along with CIGS. The performance enhancement is done by introducing a back surface field (BSF) and employing molybdenum (Mo) as a back contact. The possible effects on photovoltaic constraints of the perovskite/CIGS TFSC along with BSF have been examined by SCAPS-1D. The proposed (BaSi<sub>2</sub>/CIGS/Cs<sub>2</sub>AgBiBr<sub>6</sub>/TiO<sub>2</sub>/FTO/Mo/ Substrate) perovskite/CIGS thin film solar cell shows CE of 28.94 %. The parameters of thin film solar cell were varied for achieve optimized value which will lead to increase in efficiency. The optimized values of perovskite/CIGS TFSC were obtained that is CIGS thickness of 0.9 μm and BSF of 0.5 μm. In addition to this TFSC has been explored in terms of acceptor density, defect density and temperature of the device.

**Keywords:** Perovskite/CIGS, SCAPS-1D, Thin film solar cell

## 1 Introduction

In perovskite/CIGS thin film solar cell (TFSC) due to their simple manufacturing process and adaptability in properties, it grabbed high attention in the photovoltaic network. As a result, 2018 saw a sharp increase in its conversion efficiency (CE) of about 23% [1]. The perovskite/CIGS solar cell is basically tuned via composition and interface engineering [2]. The researchers have combined the CIGS device with perovskite and as the result, the extended bandgap results in a PCE of more than 30% [3].

CIGS solar cell achieves better performance when paired with a perovskite top cell, which has wider bandgap [4]. The thickness of CIGS layer is lowered due to its direct bandgap which enables energy utilization, allowing the foremost CIGS single-junction solar cell device to attain a CE of 23% [5]. The combination of perovskite and CIGS results in low-cost, high-performance thin-film tandem technology [6]. Moreover, the perovskite, as well as chalcogenide combinations, it can be modified by examine the optimal band-gap to enable a tandem structure. The perovskite self-dependent top model is automatically stacked on CIGS bottom model, making it a tandem solar cell with a four-terminal format [7]. The recent increase in CE of the tandem solar cells can be attributed as improvement in overall performance of perovskite/CIGS cells. It is achieved by fabrication of each sub cell separately using a less absorbent pen design, that demonstrated PCE as high as 22.1% [8]. The recent history for a 4-terminal configuration of 23.9% was announced which was made possible by expanding band gap of perovskite solar cells to 1.62 eV [8], [9].

The manufacturing of a perovskite/CIGS, on the other hand, has proven to be extremely difficult, with only a few reviews possible thus far [10]. A possible contributor is the unusual difficulty of the CIGS is its structure and shape [11]. Depending on the details of the processing, the typical lateral characteristic sizes of a CIGS layer are on the order of 500 nm to 1 μm, and the average floor root-mean-rectangular (s) roughness is in the range of 50–200 nm [12]. As a result, the most common and efficient method of



© 2023 Copyright held by the author(s). Published by AIJR Publisher in "Proceedings of the International Conference on Frontiers in Desalination, Energy, Environment and Material Sciences for Sustainable Development" (FEEMSSD-2023 & InDACON-2023). Jointly Organized by the Madan Mohan Malaviya University of Technology Gorakhpur, KIPM-College of Engineering and Technology Gida Gorakhpur, & Indian Desalination Association (InDA), India on March 16-17, 2023.

Proceedings DOI: [10.21467/proceedings.161](https://doi.org/10.21467/proceedings.161); Series: AIJR Proceedings; ISSN: 2582-3922; ISBN: 978-81-965621-8-2

perovskite production till now is the solution deposition of a perovskite top cellular [13] and it is very thin selective contacts which is impossible unless there is a significant possibility of shuffling the leading cell in tandem solar cell. With thicker PEDOT: PSS hole-particular layer in the upper and lower cells, the primary monolithic perovskite/CIGS tandem device proposed has CE of 11%. It's possible that the solar cell's performance would have been damaged by the PEDOT: PSS/perovskite interface [14], even though a much wider PEDOT: PSS layer protects the upper cell from being shunted. However, new methods are being implemented of, producing the lower cells that are competitive with monolithic tandem cells and are required to produce a green monolithic tool [15].

CIGS is known for its high efficiency, flexibility, and potential for low-cost production.

CIGS solar cell has achieved highest CE. Efficiency levels above 20% have been achieved in laboratory settings, and commercial modules typically achieve efficiencies between 15% and 20%. This makes CIGS competitive with traditional silicon-based solar cells.

Copper indium di-selenide was fabricated by spin-coating electrode deposition, which resulted in a more uniform manner. Recently, a new method was presented, similar to that employed in perovskite tandem solar cells and silicon devices, in which the topmost surface of the interconnecting layers atop the CIGS backside cells was polished to decrease roughness. [16] This allows for loss-free spin coating of solar cells and ultra-thin contact layers, which would otherwise be lost due to the roughness of the floor. Because of this, a new PCE of 22.4% was achieved [17]. However, due to the need for a very thick interconnecting layer that creates loss due to parasitic absorption, this additional polishing process may not be suitable for industrial application. Bringing the rough surface of the gadget to the top may also have a positive light trapping effect [18].

$\text{Cs}_2\text{AgBiBr}_6$ , belongs to the perovskite crystal structure family. It has a cubic crystal structure, with the caesium (Cs), silver (Ag), bismuth (Bi), and bromine (Br) atoms arranged in a specific pattern. The perovskite structure is known for its excellent optoelectronic properties and has been extensively studied for various applications.

$\text{Cs}_2\text{AgBiBr}_6$  exhibits a direct bandgap, which means that it can efficiently absorb and emit light. This property makes it suitable for optoelectronic applications, including solar cells and LEDs, where the absorption and emission of light are crucial for device performance.

This work simulates the perovskite/CIGS solar cell using SCAPS-1D tools. For this optimization, we use CIGS as first absorber layer followed by  $\text{Cs}_2\text{AgBiBr}_6$  as second absorber layer with a back surface layer of  $\text{BaSi}_2$ . The effect CIGS layer of the band gap, thickness, acceptor density, defect density, and temperature on optoelectronic parameters such as open-circuit voltage ( $V_{oc}$ ), fill factor (FF), photogenerated current density ( $J_{sc}$ ), and CE has been examined. After simulation optimized thickness of CIGS absorber layer and  $\text{BaSi}_2$  as BSF layer obtained as 0.9  $\mu\text{m}$  and 0.5  $\mu\text{m}$ , respectively, while keeping other parameters constant. The band gap of CIGS and  $\text{BaSi}_2$  are 1.1 eV and 1.3 eV, respectively. Acceptor density of CIGS absorber layer is  $10^{18}$ , defect density of CIGS absorber layer is  $10^{14}$  and optimum temperature of device is 300 K. while keeping the other parameters are constant. After simulation with back surface layer, the efficiency achieved is 28.96% with other factors such as  $V_{oc}$  of 0.85 V,  $J_{sc}$  of 42.15  $\text{mA}/\text{cm}^2$ , and FF of 80.57%.

## 2 Materials and Methods

SCAPS 1-D is a unidirectional solar cell simulation application. So many profiles like formation, recombination, and defect or other parameters of device can be calculated. The SCAPS-1D software helps us to evaluate the numerical uni-directional equations that have an impact on the conduction of charge carriers of semiconductor materials when they are in a stable state. SCAPS allows users to define various parameters related to the solar cell, such as doping concentrations, layer thicknesses, material properties,

and device geometry. These parameters can be adjusted to model different device configurations and optimize performance of solar cell.

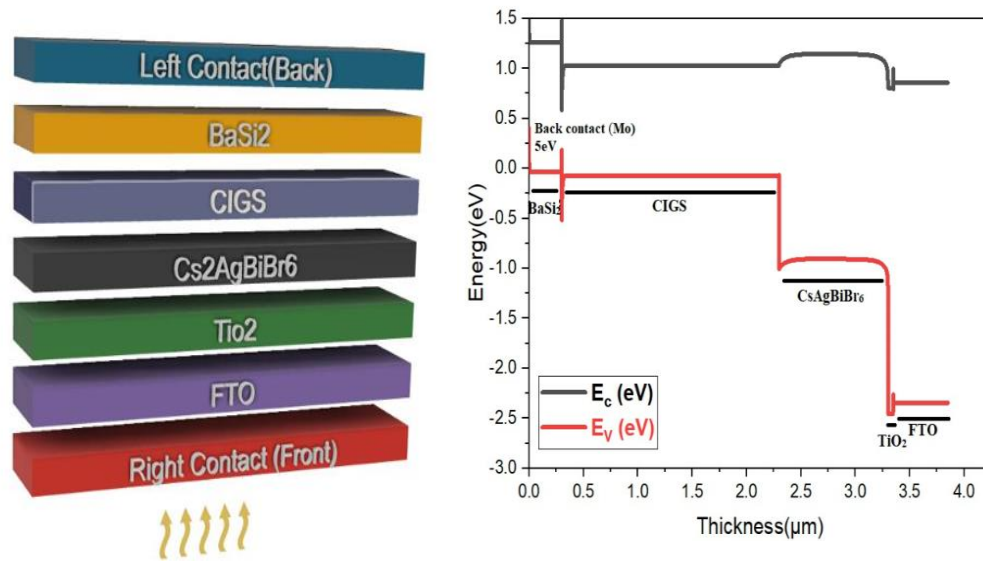


**Figure 1:** (a) Simplified formation of Proposed cell (b) energy band diagram

Fig. 1(a) shows the perovskite /CIGS TFSC proposed structure. It consists of a fluorine-doped tin oxide window layer, BaSi<sub>2</sub> which is a back surface field, CIGS and Cs<sub>2</sub>AgBiBr<sub>6</sub> as an absorber layer. The parameters and their values that are used for simulation are given in Table 1. Energy band diagram of optimize perovskite/CIGS TFSC is shown Fig. 1(b). By energy band diagram it is clearly observed that is CIGS bandgap of 1.1 eV and thickness 0.9 μm with back surface layer bandgap of 1.3 eV and thickness 0.5 μm is taken. Near zero valence band offset VBO of absorber interface is observed therefore generated holes from the absorber layer to electrode can travel smoothly.

**Table 1:** Parameters of proposed cell layer

Parameter (unit)	BaSi <sub>2</sub>	CIGS	Cs <sub>2</sub> AgBiBr <sub>6</sub>	TiO <sub>2</sub>	FTO
Thickness (μm)	0.5	0.9	1	0.05	0.5
Bandgap (eV)	1.3	1.1	2.05	3.26	3.2
Electron affinity (eV)	3.3	4.2	4.19	4.2	4.4
Conduction Band effective Density of state (cm <sup>-3</sup> )	2.6×10 <sup>19</sup>	2.2×10 <sup>18</sup>	2.2×10 <sup>18</sup>	2.0×10 <sup>17</sup>	1.8×10 <sup>19</sup>
Dielectric permittivity (relative)	11.17	13.6	5.80	9	9
Valence Band effective density of state (cm <sup>-3</sup> )	2×10 <sup>19</sup>	1.8×10 <sup>19</sup>	1.8×10 <sup>18</sup>	1.5×10 <sup>19</sup>	2.2×10 <sup>18</sup>
Hole thermal velocity (cm/s)	1×10 <sup>7</sup>	1×10 <sup>7</sup>	1×10 <sup>7</sup>	1×10 <sup>7</sup>	1×10 <sup>7</sup>
Electron thermal velocity (cm/s)	1×10 <sup>7</sup>	1×10 <sup>7</sup>	1×10 <sup>7</sup>	1×10 <sup>7</sup>	1×10 <sup>7</sup>
Hole mobility (cm <sup>2</sup> /V s)	100	25	10	25	10
Electron mobility (cm <sup>2</sup> /V s)	820	100	20	100	20
Acceptor density, N <sub>A</sub> (cm <sup>-3</sup> )	1×10 <sup>19</sup>	1×10 <sup>18</sup>	0	-	1×10 <sup>19</sup>
Donor density, N <sub>D</sub> (cm <sup>-3</sup> )	0	0	1×10 <sup>19</sup>	1×10 <sup>19</sup>	0
Defect density (cm <sup>-3</sup> )	1×10 <sup>15</sup>	1×10 <sup>14</sup>	-	1×10 <sup>14</sup>	1×10 <sup>14</sup>
Defect type	SD	SD	-	Neutral	SD

### 3 Results and Discussion

In this paper, characteristics of Perovskite/CIGS solar cell are thoroughly investigated using SCAPS-1D. Result also illuminates the effect of the back surface field ( $\text{BaSi}_2$ ) as it improves the electrical characteristics by reducing the recombination as well as more electron-hole pair generation. The consequence of varying thickness, acceptor density, defect density, and temperature of CIGS and back surface layer has been discussed. Also, the shunt and series resistance of solar cell were pre-assumed to be sure zero and enormously large, which reflect the ideal solar cell condition. Electron and hole thermal velocities are  $10^7$  cm/s. Surface recombination velocity (SVR) of hole and electron at back and front contact grid are constant to be  $10^{-7}$  cm/s. Molybdenum (Mo) having work function 5 eV is used as back contact metal.

#### 3.1 Effects of CIGS absorption layer thickness

Thickness of CIGS layer directly affects amount of light that can be absorbed by the solar cell. A thicker absorption layer allows for a higher probability of light absorption, as more photons have a chance to interact with the material. This can result in increased  $J_{sc}$  and overall CE.

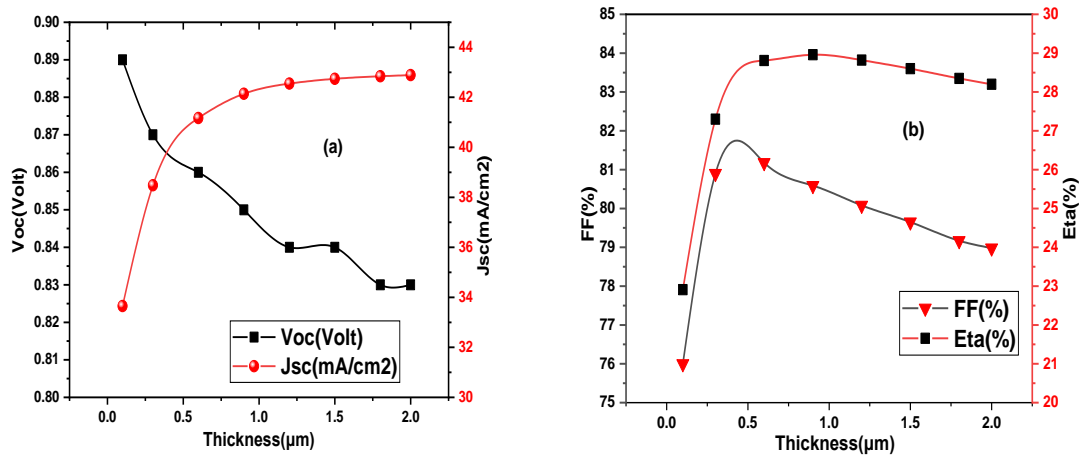


**Figure 2:** Impact of CIGS thickness variation on (a) Voc and Jsc (b) FF and efficiency.

Fig. 2 shows effect of varying thickness of CIGS layer of thin film solar cell. It is varies from 0.1  $\mu\text{m}$  to 2  $\mu\text{m}$  to examine its consequence on performance of perovskite/CIGS TFSC. In that case, optimum thickness of CIGS layer is observed 0.9  $\mu\text{m}$ . With variation of thickness from 0.1 to 2  $\mu\text{m}$ .  $J_{sc}$  increases from 30.71 to 42.14  $\text{mA}/\text{cm}^2$ , Voc fall from 0.891 to 0.85 V, the FF from 86.55% to 80.59% and the efficiency from 25.08% to 28.96%.  $J_{sc}$  increases with increasing thickness and Voc decrease with increasing in thickness.

#### 3.2 Effects of Variation of acceptor density of CIGS layer

Acceptor density of CIGS affects electronic properties and overall device performance. Varying acceptor density alters concentration of charge carriers (electrons and holes) within absorber layer. Increasing the acceptor density leads to higher hole concentrations, while decreasing the acceptor density results in lower hole concentrations. This, in turn, affects the overall device conductivity and carrier transport properties. The acceptor density of CIGS layer is changed from  $1 \times 10^{12} \text{cm}^{-3}$  to  $1 \times 10^{18} \text{cm}^{-3}$  to examine its consequence on performance of perovskite/CIGS solar cell as shown in Fig. 3. Improved fill factor and efficiency from 49.90% to 53.63% and 15.90% to 16.80% are observed. After the simulation the main conclusion was if we increase the acceptor density then the Voc, FF and efficiency will also get increased. The optimized acceptor density of CIGS is  $1 \times 10^{18} \text{cm}^{-3}$  has been observed.

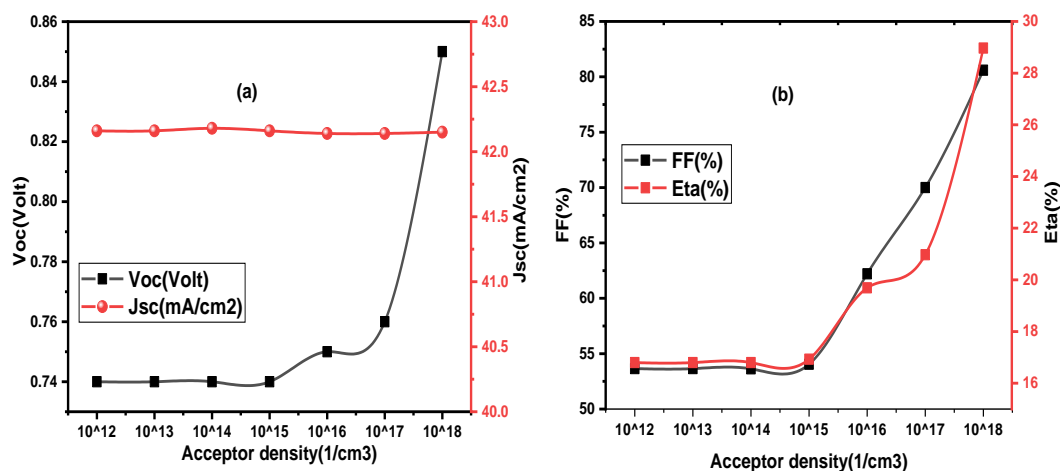


Figure 3: Impact of CIGS layer acceptor density on (a) Voc and Jsc and (b) FF and efficiency.

### 3.3 Effects of Variation of temperature of absorber layer

Temperature has significant effects on its performance and electrical characteristics. Bandgap of the absorber material is temperature dependent. As the temperature increases, the bandgap energy typically decreases. This effect can lead to a higher absorption of photons with lower energy (longer wavelength) and a shift in spectral response of the solar cell.

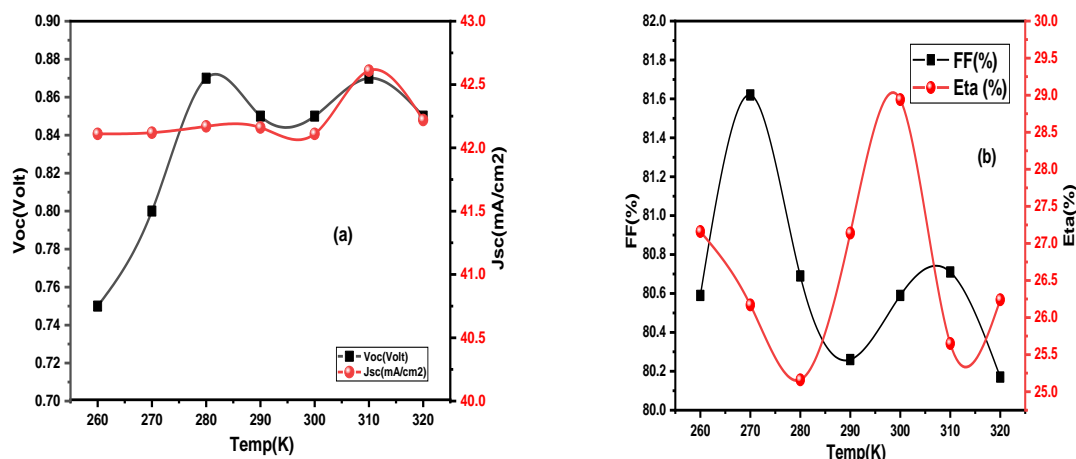


Figure 4: Impact of temperature on (a) Voc and Jsc and (b) FF and efficiency.

Solar cell is very sensitive to temperature as compared to another parameter of solar cell. For optimum performance of perovskite/CIGS solar cell depends on operating temperature of device. The temperature in the CIGS layer is increased from 260 K to 320 K to examine the effect on performance of perovskite/CIGS solar cell while keeping another parameter constant shown in Table 1. The consequence of increasing temperature is shown in Fig. 4. The consequence of changing the temperature of the CIGS absorber layer results in increase in fill factor and efficiency from 53.78% to 80.59% and 23.98% to 28.94%. Jsc get increase by increase in temperature. The optimized temperature is 300 K of operating device.

### 3.4 Effect of defect density of absorber layer

Defects within absorber layer can act as recombination centres for charge carriers (electrons and holes), leading to increased recombination rates. Higher defect densities result in more recombination events, reducing the overall efficiency of solar cell. Minimizing the defect density is crucial for maximizing carrier lifetime and minimizing recombination losses.

Absorber layer is most important layer of TFSC. Nearly all, important parameter of solar device which decides its performance enhancement occur in this section only. Hence, defect density of perovskite/CIGS material play a critical role in readjusting the density to acceptable value which is an important step for improving performance of perovskite solar cell device. Defect density of CIGS absorber layer is varied from  $1 \times 10^{12}$  to  $1 \times 10^{18}$  to examine its effect on performance of the perovskite/CIGS solar cell as shown in Fig. 5. Outcome of varying defect density results in improved fill factor and efficiency which is from 53.78% to 80.59% and 23.98% to 28.94%.

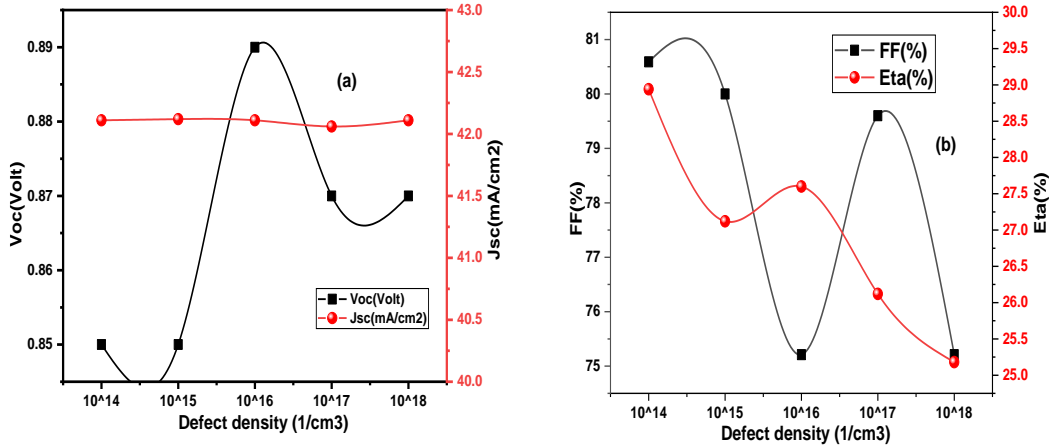


Figure 5: Impact of defect density on (a) Voc and Jsc and (b) FF and efficiency.

### 3.5 Effect of Thickness variation of BSF layer

BSF layer is designed to enhance carrier collection by creating a high electric field at back surface of TFSC. Increasing thickness of BSF layer can enhance electric field strength, promoting efficient carrier collection and reducing carrier recombination at back surface. This can lead to improved current collection and overall device efficiency.

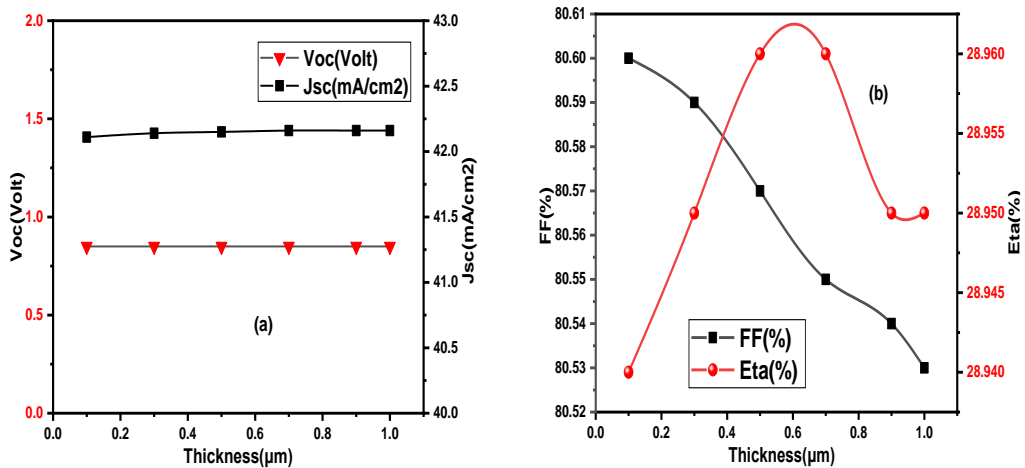


Figure 6: Impact of BSF layer thickness variation on (a) Voc and Jsc and (b) FF and efficiency.

Thickness of BSF is varies from 0.1 to 1.0 μm as shown in Fig.6. Thickness of CIGS is kept 0.9 μm, defect density  $10^{14}$  cm<sup>-3</sup>, acceptor density  $10^{18}$  cm<sup>-3</sup>, temperature 300 K and the optimize thickness of BSF layer 0.5 μm. By the variation in thickness of BSF layer from 0.1 μm to 1.0 μm after kept all the parameter are constant, we observe positive change. After analysing the performance of above parameters, we see rise in

parameters like FF, Voc, Jsc and PCE. The optimized thickness of CIGS absorber and BaSi<sub>2</sub> BSF layer achieved is 0.9  $\mu\text{m}$ , and 0.5  $\mu\text{m}$  respectively.

### 3.6 Quantum efficiency

Quantum efficiency (QE) is a measure of its capacity to convert incident photons into electric current. It describes the percentage of photons of different wavelengths (or energies) that are converted into electrical charge carriers (electrons or holes) in the solar cell.

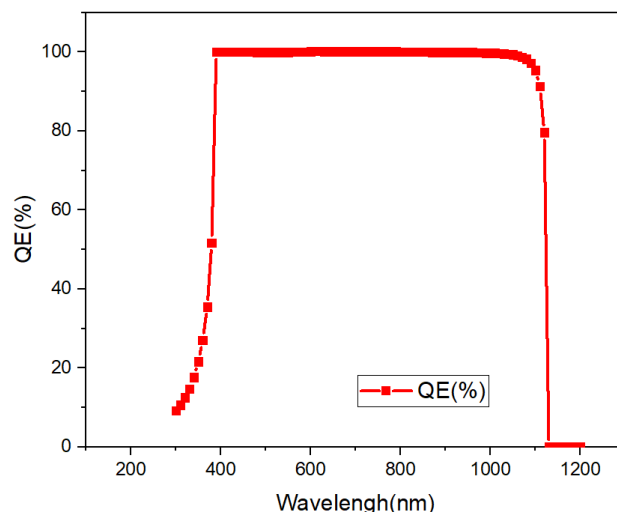


**Figure 7:** Quantum efficiency of proposed structure.

QE of perovskite/CIGS TFSC is shown in Fig.7. It shows that current will generate when illuminated by a photon of a constant wavelength. If the quantum efficiency is combined with solar electromagnetic, one can produce some value of current when introduced to the sunlight. The proportion between this highest possible energy-production value and the given energy value for the solar cell is the cell's energy conversion efficiency.

## 4 Conclusions

In this simulation we use Cs<sub>2</sub>AgBiBr<sub>6</sub> and CIGS as absorber layer along with back surface layer BaSi<sub>2</sub>. It is revealed that BaSi<sub>2</sub> layer improves performance of perovskite/CIGS TFSC of proposed structure also it is more effective material.

The above result demonstrates the effect of band gap, thickness, acceptor density, defect density and temperature on optoelectronic constraints such as FF, Voc, Jsc and PCE. The optimized value of CIGS layer, BaSi<sub>2</sub> BSF layer is 0.9  $\mu\text{m}$ , and 0.5  $\mu\text{m}$  respectively. The optimized band gap of CIGS and BaSi<sub>2</sub> is 1.1 eV and 1.3 eV respectively. The optimized value of defect density and acceptor density is the 10<sup>14</sup> cm<sup>-3</sup> and 10<sup>18</sup> cm<sup>-3</sup>. Optimized value of operating temperature of the device is 300 K. After variation in parameters the efficiency seems to be increased from 26.17% to 28.94%. The simulation work is done by using SCAPS-1D tools.

The final and optimized value of proposed perovskite/CIGS TFSC achieves CE of 28.96%, Voc of 0.85 V, Jsc of 42.15 mA/cm<sup>2</sup>, and FF of 80.57%. The record performance of TFSC displayed in this work is basic and foremost important stage toward the future enhancement of the proposed idea.

## 5 Declarations

### 5.1 Acknowledgements

The authors acknowledge Dr. Marc Burgelman at the University of Gent, Belgium, for providing the simulation software SCAPS 1-D.

### 5.2 Publisher's Note

AJIR remains neutral with regard to jurisdictional claims in institutional affiliations.

### How to Cite

Yadav et al. (2023). Performance Analysis of Perovskite/CIGS Based Thin Film Solar Cell using BaSi<sub>2</sub> as BSF Layer. *AJIR Proceedings*, 6-13. <https://doi.org/10.21467/proceedings.161.2>

### References

- [1] M. Jošt et al., 'Perovskite/CIGS Tandem Solar Cells: From Certified 24.2% toward 30% and beyond', *ACS Energy Lett*, vol. 7, no. 4, pp. 1298–1307, Apr. 2022, doi: 10.1021/ACSENERGYLETT.2C00274.
- [2] S. Yadav, P. Lohia, and A. Sahu, 'Enhanced performance of double perovskite solar cell using WO<sub>3</sub> as an electron transport material', *Journal of Optics (India)*, vol. 1, pp. 1–7, Dec. 2022, doi: 10.1007/S12596-022-01035-3.
- [3] M. B. Hosen, A. N. Bahar, M. K. Ali, and M. Asaduzzaman, 'Modeling and performance analysis dataset of a CIGS solar cell with ZnS buffer layer', *Data Brief*, vol. 14, pp. 246–250, Oct. 2017, doi: 10.1016/J.DIB.2017.07.054.
- [4] T. M. Friedlmeier et al., 'High-efficiency Cu (In,Ga)Se<sub>2</sub> solar cells', *Thin Solid Films*, vol. 633, pp. 13–17, Jul. 2017, doi: 10.1016/J.TSF.2016.08.021.
- [5] P. Chelvanathan, M. I. Hossain, and N. Amin, 'Performance analysis of copper–indium–gallium–diselenide (CIGS) solar cells with various buffer layers by SCAPS', *Current Applied Physics*, vol. 10, no. 3, pp. S387–S391, May 2010, doi: 10.1016/J.CAP.2010.02.018.
- [6] S. R. I. Biplab, M. H. Ali, M. M. A. Moon, M. F. Pervez, M. F. Rahman, and J. Hossain, 'Performance enhancement of CIGS-based solar cells by incorporating an ultrathin BaSi<sub>2</sub> BSF layer', *J Comput Electron*, vol. 19, no. 1, pp. 342–352, Mar. 2019, doi: 10.1007/S10825-019-01433-0.
- [7] T. Hossain et al., 'Tuning the bandgap of Cd<sub>1-x</sub>Zn<sub>x</sub>S (x = 0–1) buffer layer and CIGS absorber layer for obtaining high efficiency', *Superlattices Microstruct*, vol. 161, p. 107100, Jan. 2022, doi: 10.1016/J.SPML.2021.107100.
- [8] X. Li et al., 'A vacuum flash-assisted solution process for high-efficiency large-area perovskite solar cells', *Science*, vol. 353, no. 6294, pp. 58–62, Jul. 2016, doi: 10.1126/SCIENCE.AAF8060.
- [9] W. S. Yang et al., 'Iodide management in formamidinium-lead-halide-based perovskite layers for efficient solar cells', *Science* (1979), vol. 356, no. 6345, pp. 1376–1379, Jun. 2017, doi: 10.1126/SCIENCE.AAN2301
- [10] M. Kim et al., 'High-Temperature-Short-Time Annealing Process for High-Performance Large-Area Perovskite Solar Cells', *ACS Nano*, vol. 11, no. 6, pp. 6057–6064, Jun. 2017, doi: 10.1021/ACS.NANO.7B02015
- [11] T. D. Lee and A. U. Ebong, 'A review of thin film solar cell technologies and challenges', *Renewable & Sustainable Energy Reviews*, vol. 70, pp. 1286–1297, 2017, doi: 10.1016/J.RSER.2016.12.028.
- [12] S. Srivastava, A. K. Singh, P. Kumar, and B. Pradhan, 'Comparative Performance Analysis of Lead-Free Perovskites Solar Cells by Numerical Simulation', 2021, doi: 10.21203/rs.3.rs-583148/v1.
- [13] I. Alam, R. Mollick, and M. A. Ashraf, 'Numerical simulation of Cs<sub>2</sub>AgBiBr<sub>6</sub>-based perovskite solar cell with ZnO nanorod and P3HT as the charge transport layers', *Physica B Condens Matter*, vol. 618, p. 413187, Oct. 2021, doi: 10.1016/J.PHYSB.2021.413187.
- [14] M. Jošt et al., '21.6%-Efficient Monolithic Perovskite/Cu(In,Ga)Se<sub>2</sub> Tandem Solar Cells with Thin Conformal Hole Transport Layers for Integration on Rough Bottom Cell Surfaces', *ACS Energy Lett*, vol. 4, no. 2, pp. 583–590, Feb. 2019, doi: 10.1021/ACSENERGYLETT.9B00135.
- [15] T. Todorov et al., 'Monolithic Perovskite-CIGS Tandem Solar Cells via In Situ Band Gap Engineering', *Adv Energy Mater*, vol. 5, no. 23, p. 1500799, Dec. 2015, doi: 10.1002/AENM.201500799.
- [16] K. Kanchan, A. Sahu, and B. Kumar, 'Numerical Simulation of Copper Indium Gallium Diselenide Solar Cell with Ultra-Thin BaSi<sub>2</sub> Back Surface Field Layer Using the Non-Toxic In<sub>2</sub>Se<sub>3</sub> Buffer Layer', *Silicon*, vol. 14, no. 18, pp. 12675–12682, Dec. 2022, doi: 10.1007/S12633-022-01983-2.
- [17] J. Singh, U. Alam, and A. Sahu, 'Enhanced Performance of MoSe<sub>2</sub>-CIGS Solar Cell with ZnSe Buffer Layer', *Lecture Notes in Electrical Engineering*, vol. 877, pp. 705–710, 2023, doi: 10.1007/978-981-19-0312-0\_70
- [18] U. Alam and A. Sahu, 'Improved Performance of ultra-thin CIGS structure with ZnS buffer layers', *International Conference on Electrical and Electronics Engineering, ICEE 2020*, pp. 534–537, Feb. 2020, doi: 10.1109/ICEE348803.2020.9122990.